Closing in on the Mechanisms of Pulsatile Insulin Secretion

Richard Bertram,[1] Leslie S. Satin,[2] and Arthur S. Sherman[3]

Diabetes 2018;67:351–359 | https://doi.org/10.2337/dbi17-0004

Insulin secretion from pancreatic islet β-cells occurs in a pulsatile fashion, with a typical period of ∼5 min. The basis of this pulsatility in mouse islets has been investigated for more than four decades, and the various theories have been described as either qualitative or mathematical models. In many cases the models differ in their mechanisms for rhythmogenesis, as well as other less important details. In this Perspective, we describe two main classes of models: those in which oscillations in the intracellular Ca^{2+} concentration drive oscillations in metabolism, and those in which intrinsic metabolic oscillations drive oscillations in Ca^{2+} concentration and electrical activity. We then discuss nine canonical experimental findings that provide key insights into the mechanism of islet oscillations and list the models that can account for each finding. Finally, we describe a new model that integrates features from multiple earlier models and is thus called the Integrated Oscillator Model. In this model, intracellular Ca^{2+} acts on the glycolytic pathway in the generation of oscillations, and it is thus a hybrid of the two main classes of models. It alone among models proposed to date can explain all nine key experimental findings, and it serves as a good starting point for future studies of pulsatile insulin secretion from human islets.

Insulin secretion in healthy rodents, dogs, and humans is pulsatile, with mean period of ∼5 min (1). This pulsatility has been reported to enhance insulin action at the liver (2), although not all studies have shown this (3). The consequences of pulsatile insulin secretion and its dysfunction in people with or at risk for type 2 diabetes has been recently reviewed (4). The focus of this Perspective, rather, is the mechanism of insulin pulsatility, in particular the rhythmogenesis of ∼5-min oscillations in activity of pancreatic β-cells within islets of Langerhans. Although such rhythms are ubiquitous across species, we focus on mice, where most of the research on β-cell oscillations has been focused. We anticipate that over the next decade much of what we now know about mouse islets will be tested in human islets.

Pulsatility in insulin secretion reflects oscillations in the intracellular Ca^{2+} concentration of islet β-cells, which in turn reflect bursting electrical activity (5). In intact islets, several types of oscillations are commonly observed. Slow oscillations have periods typically between 4 and 6 min (Fig. 1*A*). Fast oscillations are observed in other islets, with periods typically less than 1 min (Fig. 1*B*). Fast oscillations can also be packaged into episodes to form "compound oscillations," and the episodes repeat with the same range of periods as the pure slow oscillations (Fig. 1*C*). The compound Ca^{2+} oscillations reflect a type of electrical activity called "compound bursting" (6,7). Both slow and compound Ca^{2+} oscillations have periods consistent with measurements of plasma insulin in mice (8). In human islet β-cells, most electrical oscillations reported thus far are of the fast type, but slow oscillations in the Ca^{2+} concentration have been observed (Fig. 2) and have similar periodicity to pulsatile insulin secretion (4). Human islets tend to have larger action potentials than rodent islets owing to the prominent Na^{+} currents, but the similarity of the slow oscillation periods suggests that the underlying mechanisms are similar in rodents and humans.

In the search for the biophysical mechanisms of oscillations in β-cell activity, several classes of models (both qualitative and mathematical) have emerged. We describe the key elements of these models, along with experimental findings that should be explainable by any proposed model. We conclude with a description of one recent model, the Integrated Oscillator Model (IOM), which combines features

[1]Department of Mathematics and Programs in Neuroscience and Molecular Biophysics, Florida State University, Tallahassee, FL
[2]Department of Pharmacology and Brehm Center for Diabetes Research, University of Michigan Medical School, Ann Arbor, MI
[3]Laboratory of Biological Modeling, National Institute of Diabetes and Digestive and Kidney Diseases, National Institutes of Health, Bethesda, MD
Corresponding author: Richard Bertram, bertram@math.fsu.edu.

Received 2 August 2017 and accepted 30 November 2017.

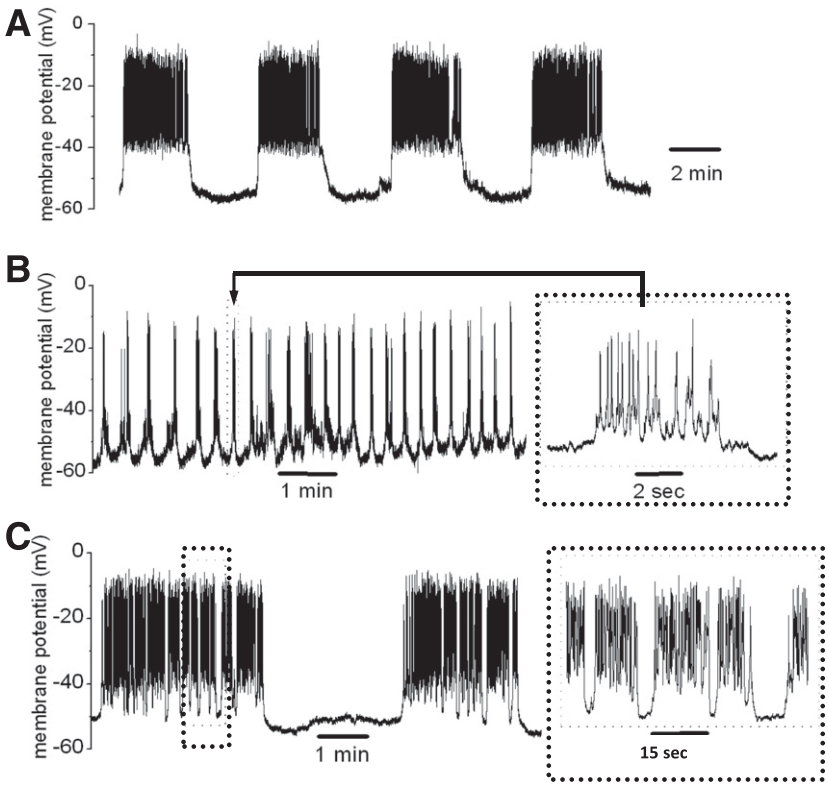

Figure 1—Intracellular electrical recordings from islet β-cells exhibiting three types of oscillations. *A*: Example of islet with slow oscillations. *B*: An islet exhibiting fast oscillations. *C*: An islet with compound oscillations composed of episodes of fast oscillations. Recordings were made using perforated patch and amphotericin B. Ren and Satin, unpublished data.

of prior models and satisfies all the experimental tests described herein.

We focus on the interactions of Ca^{2+} and metabolism in generating slow oscillations, omitting discussion of other interesting areas that have been the subject of mathematical modeling (as in Fridlyand et al. [9]), such as cAMP oscillations, synchronization within and among islets, and exocytosis. Some have suggested that other factors, such as cAMP, islet paracrine factors, and insulin itself may play roles in β-cell oscillations, but because of space restrictions we do not discuss these hypotheses.

HYPOTHESES FOR ISLET OSCILLATIONS

In 1983 Chay and Keizer (10) published a pioneering β-cell model that spawned many subsequent models. At its core was slow negative feedback, a ubiquitous mechanism for oscillations, whereby a rise in intracellular free Ca^{2+} activates Ca^{2+}-activated K^+ channels (K_{Ca} channels). According to this model, the rise of intracellular Ca^{2+} during a burst active phase and its decline during a silent phase drives bursting through its action on K_{Ca} channels. This model was successful at reproducing the fast (i.e., 15-s period) burst pattern predominantly reported in the literature at the time, as well as the response of the cell to changes in glucose. That is, at low glucose levels the cell is silent, at higher levels it bursts, and at the highest levels it produces a continuous train of impulses. Within the bursting regimen, increases in the glucose level increase the active phase duration relative to the silent phase duration, known as the "plateau fraction."

Shortly after the publication of this model, ATP-sensitive K^+ channels (K_{ATP} channels) were first reported in β-cells (11). The importance of these channels in setting insulin secretion to a level appropriate for the prevailing blood glucose concentration was immediately recognized, but their existence also raised the possibility that oscillations in metabolism could underlie oscillations in the cells' electrical activity, Ca^{2+} level, and insulin secretion. Indeed, there have been numerous subsequent measurements of metabolic oscillations in islets, including oscillations in oxygen consumption, NAD(P)H, and mitochondrial membrane potential, as reviewed in Bertram et al. (12).

The two main classes of models for β-cell oscillations can be categorized into those in which oscillations in Ca^{2+} drive oscillations in metabolism (Ca^{2+}-driven oscillations) and those in which oscillations in metabolism drive oscillations in Ca^{2+} (metabolism-driven oscillations). The many models constituting the first class differ in the specific biophysical components most important for electrical activity and Ca^{2+} oscillations. In all cases, however, bursting electrical activity (Fig. 3*A*) reflects slow negative feedback through one or more slow processes that we represent by a single slow

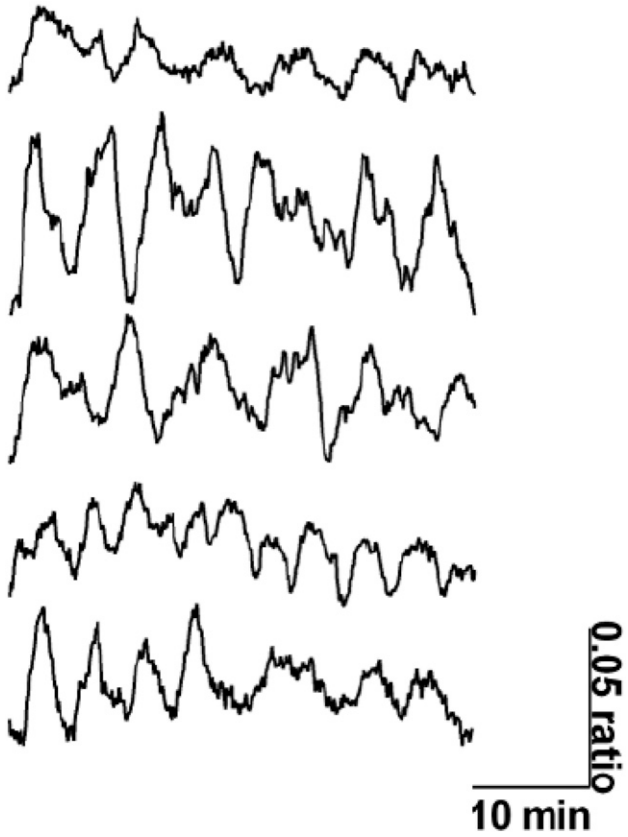

Figure 2—Oscillations in intracellular Ca^{2+} concentration in five different human islets loaded with the ratiometric dye Fura-PE3 AM. All show slow oscillations, similar to what is often observed in mouse islets.

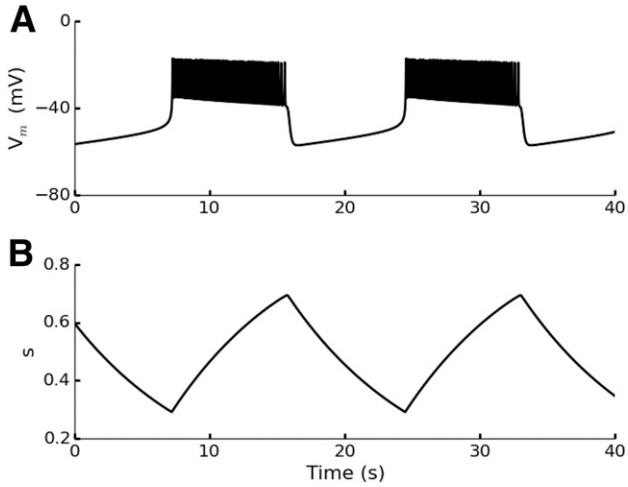

Figure 3—Computer simulations of a model in which bursting electrical activity is driven by activity-dependent variation in a slow process *s*. *A*: Electrical bursting, characterized by periodic active phases of spiking and silent phases of membrane hyperpolarization. *B*: Sawtooth time course of *s*.

variable *s*. During the active phase, *s* slowly rises and ultimately terminates spiking, while during the silent phase it slowly declines, eventually becoming small enough for electrical activity to begin again. This variable therefore has a sawtooth time course (Fig. 3*B*). In some models, metabolic oscillations occur as a result of Ca^{2+}-dependent ATP production (13,14) or Ca^{2+}-dependent ATP consumption by Ca^{2+} pumps (15–17). In other variants, the slow negative feedback that drives bursting is not provided directly by Ca^{2+} but by voltage-dependent inactivation of Ca^{2+} channels (13,18) or by the accumulation of Na^+, possibly mediated by the Na^+/Ca^{2+} exchanger, which in turn activates Na^+/K^+ pumps (16,17) or a combination of ionic mechanisms (17,19). In all these cases, however, the metabolic oscillations are due to oscillations in Ca^{2+}.

The alternative idea that metabolic oscillations drive Ca^{2+} oscillations in β-cells was first proposed by Tornheim (20), based on the observation that oscillations in glycolysis can be measured in muscle extracts (21) and are due to the muscle isoform (PFK-M) of the key glycolytic enzyme phosphofructokinase (PFK). In this step, fructose 6-phosphate (F6P) is converted to fructose 1,6-bisphosphate (FBP), which is an allosteric activator of PFK-M activity. This same isoform is present in β-cells and is the most active PFK isoform (22). The hypothesis is that glycolytic oscillations occur in glucose-stimulated β-cells and that these lead to oscillations in ATP production, which modulates K_{ATP} channels, driving electrical bursting and Ca^{2+} oscillations. This is the template for the second general class of models.

The Dual Oscillator Model (DOM) combines elements of the two major classes and postulates that Ca^{2+} oscillations drive the fast electrical bursting in β-cells, while glycolytic oscillations, when active, drive slow bursting (12). Compound bursting is driven by both processes, the fast bursts within an episode being driven by Ca^{2+} feedback onto K_{Ca} channels, whereas the pacing of the episodes is controlled by glycolytic oscillations and ATP/ADP action on K_{ATP} channels. The model was recently modified to add negative feedback of Ca^{2+} onto the metabolic pathway (23). This change improved agreement between our newer experimental observations while preserving the previous advantages of the DOM. The joint participation of Ca^{2+} feedback and glycolysis in slow oscillations, which makes the model neither purely Ca^{2+}-driven nor metabolism-driven, motivates the name "Integrated Oscillator Model."

KEY EXPERIMENTAL FINDINGS

Table 1 lists experimental findings that provide particularly useful constraints for biophysical models of oscillatory islet activity. The first three rows of Table 1 indicate which models can account for fast, slow, and compound oscillations. (Two models [15,20] are qualitative rather than mathematical models, so we have to infer the behaviors they could produce.) Compound oscillations are the most challenging to explain and are most robustly accounted for by models which have metabolism-driven oscillations as well as Ca^{2+} feedback onto K^+ channels (the DOM and IOM).

Table 1—Key experimental findings and the models that can replicate them

	Models with Ca^{2+}-driven oscillations	Models with metabolism-driven oscillations
Fast bursting and Ca^{2+} patterns	CK83, KM89, SK92, D98, F03, BS04, C11, Dd06	DOM, IOM
Slow bursting and Ca^{2+} patterns	D98, BS04, C11, Dd06	T97, DOM, IOM
Compound bursting and Ca^{2+} patterns	B08	DOM, IOM
Subthreshold oscillations	None	T97, DOM, IOM
Metabolic oscillations with Ca^{2+} clamped by Dz	None	DOM, IOM
Oscillations in K_{ATP} conductance measured with voltage ramps during islet bursting	None	T97, DOM, IOM
Ca^{2+} oscillations stimulated by KIC	CK83, KM89, SK92, D98, F03, BS04, C11, Dd06	IOM
Sawtooth oscillations in Perceval	CK83, KM89, SK92, D98, F03, BS04, C11, Dd06	IOM
Sawtooth oscillations in PKAR	None	IOM

B08, Bertram et al., 2008 (48); BS04, Bertram and Sherman, 2004 (49); C11, Cha et al., 2011 (17); CK83, Chay and Keizer, 1983 (10); D98, Detimary et al., 1998 (15); Dd06, Diederichs, 2006 (50); DOM, Bertram et al., 2007 (27); F03, Fridlyand et al., 2003 (16); IOM, McKenna et al., 2016 (23); KM89, Keizer and Magnus, 1989 (40); SK92, Smolen and Keizer, 1992 (13); T97, Tornheim, 1997 (20).

The next experimental finding (row 4, Table 1) is oscillations in K_{ATP} conductance (24) or Ca^{2+} concentration (25) seen in the presence of subthreshold glucose concentrations. In this case, the K_{ATP} conductance is too large to allow action potentials, but small oscillations in the membrane potential can sometimes be observed (Thompson and Satin, unpublished data). The data cited suggest that metabolic oscillations can occur at low glucose, which implies that oscillations in metabolism, and concomitant small amplitude oscillations in Ca^{2+}, do not require electrical bursting oscillations.

A direct way to discriminate between Ca^{2+}-driven metabolic oscillations and metabolism-driven Ca^{2+} oscillations is to clamp one of the two variables and determine whether the other still oscillates. Clamping cytosolic Ca^{2+} has been done using diazoxide (Dz), which opens K_{ATP} channels and thereby hyperpolarizes β-cells (row 5, Table 1). It was found that the metabolic oscillations present in stimulatory glucose were terminated by the application of Dz (26,27), which suggested that metabolic oscillations require Ca^{2+} oscillations. It was later shown that metabolic oscillations can in fact persist under these conditions in some islets (i.e., in Dz and without Ca^{2+} oscillations) and that even in islets where Dz initially abrogates the metabolic oscillations they can often be rescued by elevating Ca^{2+} by adding KCl to Dz to depolarize the islet while Ca^{2+} remains steady (Fig. 4) (28).

Another way to clamp the Ca^{2+} level of a β-cell in an islet is to use patch clamping to fix the membrane potential (row 6, Table 1). In stimulatory glucose, the rest of the islet will continue to exhibit electrical activity while the patched cell is held at the clamp command potential. In Ren et al. (29), voltage ramps were used to generate current-voltage curves from the patched cell while the rest of the islet displayed slow bursting electrical activity. Analysis of the data revealed slow oscillations in K_{ATP} conductance, with lower conductance during the active phases of the bursts than during the silent phases (Fig. 5). The K_{ATP} oscillations likely resulted from metabolic oscillations in the clamped cells, as the Ca^{2+} level was nonoscillatory because of the voltage clamp. As seen in Fig. 5*B*, the K_{ATP} conductance has a square shape rather than the sawtooth shape in Fig. 3*B*, indicating that the metabolic oscillations occurred in pulses under these conditions.

An alternative to clamping Ca^{2+} is to clamp metabolism and determine whether electrical bursting and Ca^{2+} oscillations persist. This has been attempted using the fuel α-ketoisocaproic acid (KIC), which enters metabolism at the citric acid cycle, bypassing glycolysis (row 7, Table 1). Some studies have shown that KIC can induce Ca^{2+}

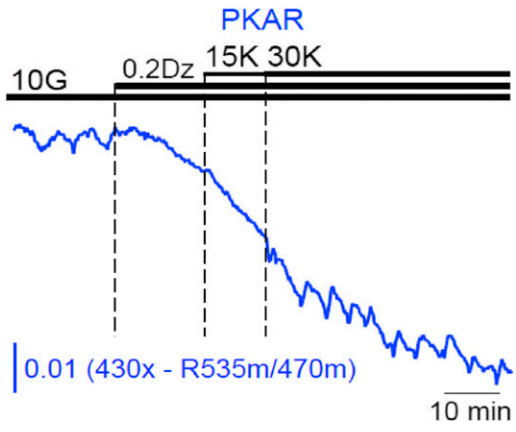

Figure 4—Measurement of PKAR, which reflects dynamics in the FBP concentration. The islet is initially exposed to 10 mmol/L glucose (G), then 0.2 mmol/L Dz is added, and finally KCl (K) is added. Oscillations that are eliminated by the Dz are rescued by depolarization when the KCl concentration is increased from 15 to 30 mmol/L. Reprinted with permission from Merrins et al. (35).

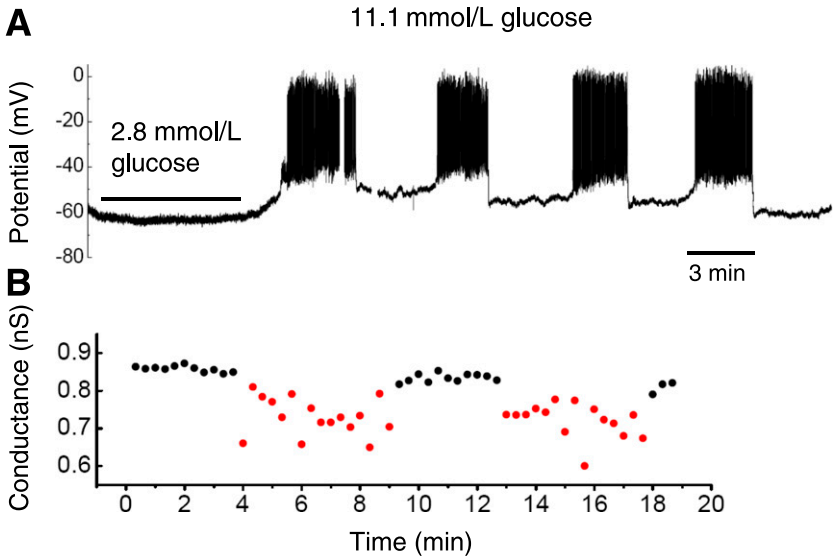

Figure 5—Measurement of the K_{ATP} channel conductance made from a patched cell in an islet exposed to 11.1 mmol/L glucose. *A*: Slow bursting produced when the patch electrode is in current clamp mode. *B*: K_{ATP} channel conductance when the patch electrode is in voltage clamp mode with the application of rapid voltage ramps (2-s ramps from −120 mV to −50 mV). Red symbols identify the conductance during the active phases of two bursts; there are clear pulses of reduced conductance during the bursts. Panels *A* and *B* are sequential, not aligned. Protocol similar to that used in Ren et al. (29). nS, nanosiemens.

oscillations with period of several minutes, even in the absence of glucose; these oscillations are qualitatively similar to those induced by glucose alone (30,31). This observation is not universal, however, as Ca^{2+} oscillations were not observed in two studies that used the same KIC concentration (32,33). In the cases where KIC-induced Ca^{2+} oscillations were observed, they could not have resulted from glycolytic oscillations. Although these data pose no challenge to the class of models with Ca^{2+}-induced metabolic oscillations, they are a substantial challenge to models in which Ca^{2+} oscillations are driven by metabolic oscillations. Recently, however, it was demonstrated that the IOM can account for KIC-induced Ca^{2+} oscillations (23) caused by the utilization of ATP by Ca^{2+} pumps, which is the mechanism described by Detimary et al. (15) and above. This differs from glucose-induced oscillations in the IOM, which are driven primarily by the glycolytic subsystem and Ca^{2+} feedback onto mitochondrial dehydrogenases, as explained below. Note that the predicted shapes of ATP and Ca^{2+} are very similar for these two mechanisms, so it is difficult to know which mechanism is driving the oscillations without simultaneously measuring a glycolytic metabolite.

A real-time fluorescent readout of the ATP time course has been made using the ATP-sensing fluoroprotein Perceval or its improved variant Perceval-HR (34). These studies showed that the ATP/ADP ratio in the cytosol (35) or submembrane space of the β-cells (36) exhibited sawtooth oscillations in response to stimulatory glucose (row 8, Table 1). A slow decline in ATP/ADP was observed throughout the active phase of the burst and a slow rise during the silent phase. This would be expected if oscillations are driven by the mechanism proposed in Detimary et al. (15). During the active phase, Ca^{2+} is elevated, so ATP slowly declines as a result of hydrolysis by Ca^{2+} ATPase pumps, in turn reactivating the K_{ATP} channels. During the silent phase, Ca^{2+} is low, so ATP slowly rises, inhibiting K_{ATP} channels and ultimately starting a new active phase. The IOM, which includes this mechanism, can also account for the sawtooth shape of ATP/ADP (23).

The final row of Table 1 refers to an experimental study that used a Förster resonance energy transfer biosensor (pyruvate kinase activity reporter, or PKAR [37]) that is sensitive to FBP to monitor the time course of the product of the key glycolytic enzyme PFK-M. PKAR, a direct probe of glycolytic oscillations, was found to oscillate in glucose-stimulated islets with a sawtooth pattern (37). Moreover, simultaneous measurements of PKAR and membrane potential (Fig. 6*A*) or Ca^{2+} revealed that PKAR (and thus FBP) typically declines during the burst active phase and rises during the silent phase (35). Such FBP oscillations would not be predicted by models in which metabolic oscillations are driven by Ca^{2+} feedback downstream of glycolysis. The DOM, which is based on intrinsic slow glycolytic oscillations, also failed to account for the sawtooth pattern of the FBP oscillations or their phase relationship to Ca^{2+} oscillations (35). This deficiency was overcome in the IOM by incorporating Ca^{2+} stimulation of pyruvate dehydrogenase, as we discuss next. Although a sawtooth PKAR pattern was most common, a subset of islets exhibited more pulsatile PKAR oscillations (Fig. 6*B*), which is also consistent with the IOM (Fig. 7*H* and McKenna and Bertram [unpublished data]).

THE INTEGRATED OSCILLATOR MODEL

The IOM builds on the DOM by adding a key Ca^{2+} feedback to glycolysis (23). Glucose metabolism involves several

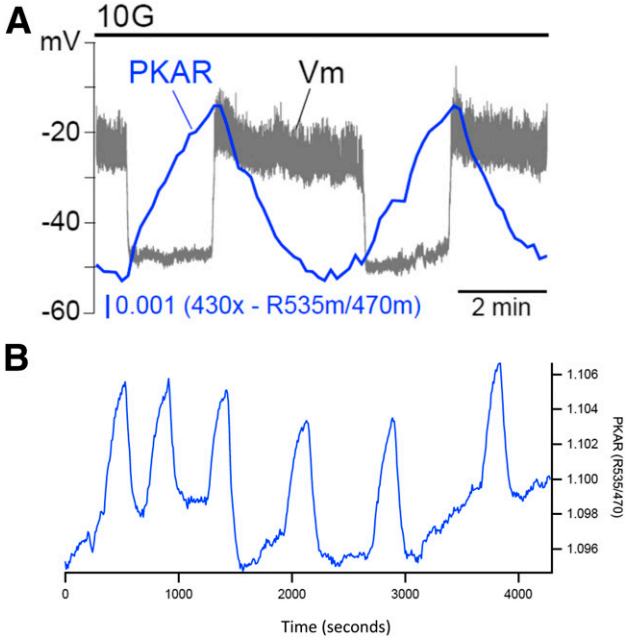

Figure 6—PKAR measurements from two bursting islets with very different time courses. *A*: Sawtooth PKAR time course, measured simultaneously with the membrane potential from a patched cell. *B*: Pulsatile PKAR time course.

Ca^{2+}-activated dehydrogenases involved in the production of NADH and $FADH_2$. In particular, pyruvate dehydrogenase (PDH), which converts pyruvate to acetyl-CoA and immediately precedes the citric acid cycle, is strongly activated by Ca^{2+} (38). We describe next how this Ca^{2+} feedback impacts glycolysis to shape the time course of FBP and ATP in the model.

In the DOM, glycolytic oscillations are driven by feedback of the product FBP onto its synthetic enzyme, PFK-M. This positive feedback results in the regenerative production of FBP until its precursor, F6P, becomes substantially depleted. This depletion greatly reduces FBP production until the substrate has built up again. This process of growth, decline, and renewal results in oscillations having a period of ~5 min (39). Glucose is the primary input to the system; if it is low, the rate of FBP production will be too low to produce glycolytic oscillations (Fig. 7*A*). If the glucose level is too high, then F6P will not be depleted, so FBP production will be high and nonoscillatory (Fig. 7*C*). Only at intermediate values will slow oscillations occur (Fig. 7*B*), and the FBP time course will be pulsatile. The top row of Fig. 7 schematizes the control of the glycolytic oscillator by glucose influx in the DOM. In Fig. 7*A–C* the box shown represents glycolysis, including the positive feedback of FBP on PFK-M, and the glucose level (or influx of F6P) is represented by the width of the input channel to glycolysis. The output of glycolysis, pyruvate, is ultimately metabolized in the mitochondria to form ATP, which inhibits PFK-M and hence lowers the rate of glycolysis, as indicated in Fig. 7. ATP also closes K_{ATP} channels, as indicated, and its concentration is reduced by Ca^{2+} owing to Ca^{2+} pump hydrolysis (15).

In the DOM, we did not consider the effect of the glycolytic efflux rate on the glycolytic oscillations, but it is as important as the effect of the glycolytic influx rate. Thus, if the output of the glycolytic pathway is constricted, as illustrated in Fig. 7*D*, then the FBP concentration will build up, which would terminate glycolytic oscillations, similar to the case of high glucose influx (Fig. 7*C*), but termination now occurs because of excessive positive feedback by FBP. At the other extreme, if the efflux rate is very high (Fig. 7*F*), then the FBP generated by PFK-M would be quickly metabolized, resulting in low FBP and thus insufficient positive feedback onto PFK-M. There would again be no glycolytic oscillations, similar to the case of low glucose influx (Fig. 7*A*); with high glycolytic efflux, however, ATP production would be large, whereas with low glucose ATP production would be small.

In the IOM, Ca^{2+} regulates glycolytic efflux through its stimulation of PDH, as indicated by the gray shadowing in Fig. 7*G*. When cytosolic Ca^{2+} is low, glycolytic efflux will be reduced (solid channel in Fig. 7*G*), causing FBP to accumulate. When Ca^{2+} is high, glycolytic efflux will be high (gray channel in Fig. 7*G*), causing FBP to decline. When Ca^{2+} oscillates, FBP will have a sawtooth-shaped time course, rising during the down phase of a Ca^{2+} oscillation when FBP efflux is low and declining during the up phase when FBP efflux is high, in agreement with the PKAR data shown in Fig. 6*A* (row 9 of Table 1). Downstream ATP production will inherit this time course, rising when Ca^{2+} is low and falling when Ca^{2+} is high, in agreement with Perceval and Perceval-HR measurements (row 8 of Table 1). Even though both the Ca^{2+} hydrolysis mechanism (15) and the inhibition of ATP production by mitochondrial Ca^{2+} influx (40) can also account in a natural way for the sawtooth time course of ATP, neither can account for the sawtooth time course of FBP. While there is also evidence for positive feedback of Ca^{2+} on glycolysis at glucokinase (41), this would not yield the observed sawtooth shape of FBP.

Although the IOM generates sawtooth-shaped FBP and ATP oscillations when Ca^{2+} is free to oscillate, pulses of FBP and ATP are predicted when Ca^{2+} is not freely oscillating. For example, at low glucose there should be minimal electrical activity, so Ca^{2+} should be low with perhaps small fluctuations. Although glycolytic oscillations do not typically occur in low glucose in which there is no bursting electrical activity, in some cases they appear to do so, resulting in pulses of FBP and ATP (12,25). Whereas FBP pulses have not yet been observed experimentally in substimulatory glucose, evidence for ATP oscillations have been observed indirectly (row 4 of Table 1) through recordings of K_{ATP} channel activity (24). Ca^{2+} oscillations are also prohibited when a β-cell in an islet is voltage-clamped in stimulatory glucose (as in Ren et al. [29]), but, as described above, we observed the pulse-shaped K_{ATP} channel conductance oscillations predicted by the IOM (row 6 of Table 1 and Fig. 5).

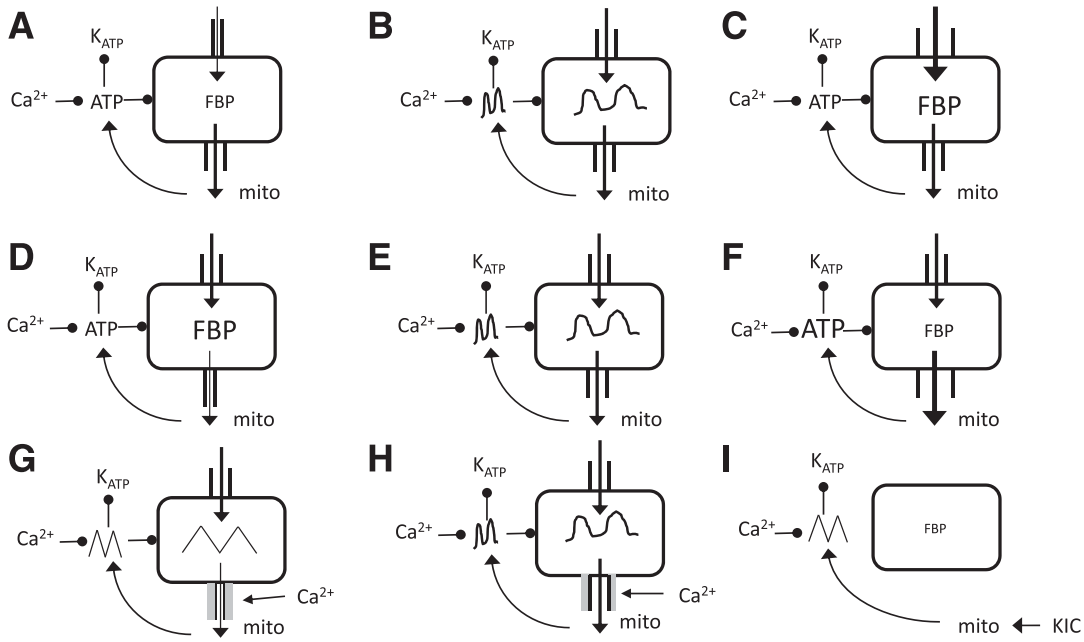

Figure 7—Effects of glycolytic input and output on FBP and ATP. *A–F*: DOM; *G–I*: IOM. In each panel, the box represents the core glycolytic oscillator, in which positive feedback of FBP on PFK supplies the drive. *A*: With low glucose influx, both FBP and ATP levels are low and steady. *B*: With intermediate glucose influx, pulsatile oscillations of FBP result. *C*: With high glucose influx, both FBP and ATP levels are high and steady. *D*: With moderate glucose influx and low glycolytic efflux, the FBP level will be high but the ATP level will be low. *E*: Glycolytic oscillations can occur with moderate glucose influx and moderate glycolytic efflux, resulting in pulses of FBP and ATP, as in panel *B*. *F*: With moderate glucose influx and high glycolytic efflux, FBP is low but ATP level is high. *G*: In the IOM, Ca^{2+} modulates the glycolytic efflux through stimulation of PDH. With low Ca^{2+} glycolytic efflux is low (black output channel), and with high Ca^{2+} it is high (gray output channel). This results in sawtooth-shaped FBP and ATP time courses. *H*: The IOM can produce pulsatile FBP oscillations if the basal efflux is in the permissive intermediate range. *I*: The fuel KIC enters metabolism in the citric acid cycle, downstream of glycolysis. Oscillations in ATP and Ca^{2+} can occur due to the hydrolysis of ATP that powers Ca^{2+} pumps. Other models in which Ca^{2+} drives metabolic oscillations can account for this, but not for any of the other panels. Thicker arrows indicate greater flux.

In an informative experiment, Ca^{2+} was clamped in the entire islet by Dz and subsequently elevated by KCl, but we saw NAD(P)H oscillations (28). We also observed NAD(P)H oscillations in $SUR1^{-/-}$ islets lacking Ca^{2+} oscillations (28), providing further evidence that metabolic oscillations can occur without Ca^{2+} oscillations (row 5 of Table 1 and Fig. 4).

In the IOM, the application of Dz to normal islets would lower cytosolic Ca^{2+} concentration, constricting the efflux from glycolysis, which would increase FBP (Fig. 7*D*). However, low Ca^{2+} would also increase ATP as a result of reduced Ca^{2+} pumping, so that PFK-M would be partially inhibited. This would have the opposite effect on the FBP concentration, causing it to decrease. The competition between these opposing actions was clearly shown using PKAR (35); Dz in stimulatory glucose raised PKAR activity initially to a plateau, indicating elevated cytosolic FBP, followed by a decline. When KCl was added later, increasing intracellular Ca^{2+}, the PKAR signal quickly declined, indicating the dominance of the Ca^{2+}-induced increase in glycolytic efflux (as in Fig. 7*F*).

The IOM also accounts for our observation of pulsatile PKAR even when Ca^{2+} is unclamped, much like the original DOM. This can happen in the model if glycolytic efflux is in the permissive intermediate regimen when Ca^{2+} is low (Fig. 7*H*). Unlike the DOM, the efflux rate oscillates with Ca^{2+} in the IOM, but glycolytic oscillations dominate, resulting in pulsatile FBP.

Figure 7*I* illustrates the effect of the fuel KIC, which enters metabolism in the citric acid cycle. When applied in the absence of glucose the glycolytic pathway is bypassed, illustrated by a very low level of FBP. KIC increases ATP production, elevating the ATP level and closing K_{ATP} channels. Ca^{2+} feedback on ATP consumption (15) or production (40) can then produce electrical bursting and Ca^{2+} oscillations (row 7 of Table 1) that are totally independent of glycolysis (23). Other models in which metabolic oscillations are driven by Ca^{2+} oscillations similarly predict ATP oscillations in response to KIC but do not account for metabolic oscillations in the absence of Ca^{2+} oscillations.

SUMMARY AND CONCLUSIONS

There appear to be several mechanisms for slow and compound Ca^{2+} oscillations, which correspond to the observed ~5 min period of plasma insulin oscillations. The IOM suggests that the metabolic oscillations seen when Ca^{2+} is clamped are due to intrinsic glycolytic oscillations driven by the allosteric enzyme PFK-M. When Ca^{2+} is not clamped, the IOM suggests that metabolic, Ca^{2+}, and electrical oscillations again involve the glycolytic pathway, but in this case

Ca^{2+} feedback onto glycolytic output, through activation of pyruvate dehydrogenase, is responsible for the sawtooth pattern observed in FBP, as assessed by the Förster resonance energy transfer sensor PKAR. A third oscillation mechanism appears operative when the fuel KIC is used with little or no glucose, preventing glycolytic oscillations; here the hydrolysis of ATP to power Ca^{2+} pumps is the key controlling element. The IOM suggests (23) that a similar nonglycolytic mechanism may also be responsible for the slow Ca^{2+} oscillations that have been reported in islets from PFK-M knockout mice (42).

Why are there so many mechanisms for slow oscillations? As insulin pulsatility is important for insulin's downstream targets, the system may have evolved to include redundancy to maintain pulsatility. It is noteworthy that when slow Ca^{2+} oscillations have been seen in KIC in the absence of glucose, their periods have been very similar to the oscillations seen in glucose alone (30). This suggests that the various mechanisms are part of an integrated system organized to produce the canonical 5-min period independent of fuel availability; it is difficult to see how independent pathways would produce the same result.

We believe the field is closing in on a comprehensive model of slow oscillations. We acknowledge, however, that while the IOM can account for the key experimental observations, many of its details await experimental verification. Although there is good evidence that a rise in Ca^{2+} is sufficient to reduce ATP (36), we lack quantitative data proving that ATP depletion is sufficient to mediate the role ascribed to it in the model. Tests to perturb mitochondrial Ca^{2+} uptake are needed to ascertain whether the assumed effects occur and are of appropriate magnitude to mediate their claimed functions. Not all studies have found the expected increase in NAD(P)H and $FADH_2$ by Ca^{2+} (43); the coexistence of positive and negative sites of Ca^{2+} action can lead to diverse responses that are difficult to disentangle. The prediction mentioned earlier of metabolic oscillations during subthreshold Ca^{2+} oscillations awaits confirmation, and the relative prevalence of pulse- and sawtooth-shaped oscillations of FBP remains to be systematically investigated. Metabolic oscillations are synchronized across islets (37), but it is not known whether this is mediated by diffusion of metabolites across gap junctions or secondarily to synchronization of membrane potential and Ca^{2+}. The mechanisms underlying observations of slow Ca^{2+} oscillations in islets lacking K_{ATP} channels (44,45) are also not yet established, but a compensation mechanism has been suggested (46); oscillations have been reported to occur in some islets deprived of K_{ATP} channels for only 20 min, so compensation may be more rapid than previously appreciated (47). Finally, our focus on the slow oscillations leaves unclear the physiological significance of the fast oscillations.

The progress detailed here in rodents provides a framework to investigate the applicability of the model to human islets. Although there is considerable evidence for disturbed pulsatility in type 2 diabetes in humans, as reviewed by Satin et al. (4), further study of the relative contributions of altered patterning and reduced β-cell mass to secretion is called for. The challenge ahead is to efficiently use our accumulated knowledge of mouse islets to understand the oscillations in the more important (to us) human islets and identify new therapeutic targets that can restore normal pulsatile patterns to patients with type 2 diabetes.

Funding. R.B. was supported by a grant from the National Science Foundation (DMS-1612193), L.S.S. by a grant from the National Institutes of Health National Institute of Diabetes and Digestive and Kidney Diseases (NIDDK) (R01-DK46409), and A.S.S. by the Intramural Research Program of the National Institutes of Health (NIDDK).

Duality of Interest. No potential conflicts of interest relevant to this article were reported.

References

1. Song SH, McIntyre SS, Shah H, Veldhuis JD, Hayes PC, Butler PC. Direct measurement of pulsatile insulin secretion from the portal vein in human subjects. J Clin Endocrinol Metab 2000;85:4491–4499

2. Matveyenko AV, Liuwantara D, Gurlo T, et al. Pulsatile portal vein insulin delivery enhances hepatic insulin action and signaling. Diabetes 2012;61:2269–2279

3. Grupert JM, Lautz M, Lacy DB, et al. Impact of continuous and pulsatile insulin deliver on net hepatic glucose uptake. Am J Physiol Endocrinol Metab 2005;289: E232–E240

4. Satin LS, Butler PC, Ha J, Sherman AS. Pulsatile insulin secretion, impaired glucose tolerance and type 2 diabetes. Mol Aspects Med 2015;42:61–77

5. Nunemaker CS, Satin LS. Episodic hormone secretion: a comparison of the basis of pulsatile secretion of insulin and GnRH. Endocrine 2014;47:49–63

6. Cook DL. Isolated islets of Langerhans have slow oscillations of electrical activity. Metabolism 1983;32:681–685

7. Henquin JC, Meissner HP, Schmeer W. Cyclic variations of glucose-induced electrical activity in pancreatic B cells. Pflugers Arch 1982;393:322–327

8. Nunemaker CS, Zhang M, Wasserman DH, et al. Individual mice can be distinguished by the period of their islet calcium oscillations: is there an intrinsic islet period that is imprinted in vivo? Diabetes 2005;54:3517–3522

9. Fridlyand LE, Tamarina N, Philipson LH. Bursting and calcium oscillations in pancreatic β-cells: specific pacemakers for specific mechanisms. Am J Physiol Endocrinol Metab 2010;299:E517–E532

10. Chay TR, Keizer J. Minimal model for membrane oscillations in the pancreatic β-cell. Biophys J 1983;42:181–190

11. Ashcroft FM, Harrison DE, Ashcroft SJH. Glucose induces closure of single potassium channels in isolated rat pancreatic β-cells. Nature 1984;312:446–448

12. Bertram R, Sherman A, Satin LS. Metabolic and electrical oscillations: partners in controlling pulsatile insulin secretion. Am J Physiol Endocrinol Metab 2007;293: E890–E900

13. Smolen P, Keizer J. Slow voltage inactivation of Ca^{2+} currents and bursting mechanisms for the mouse pancreatic beta-cell. J Membr Biol 1992;127:9–19

14. Magnus G, Keizer J. Model of β-cell mitochondrial calcium handling and electrical activity. I. Cytoplasmic variables. Am J Physiol 1998;274:C1158–C1173

15. Detimary P, Gilon P, Henquin JC. Interplay between cytoplasmic Ca^{2+} and the ATP/ADP ratio: a feedback control mechanism in mouse pancreatic islets. Biochem J 1998;333:269–274

16. Fridlyand LE, Tamarina N, Philipson LH. Modeling of Ca^{2+} flux in pancreatic β-cells: role of the plasma membrane and intracellular stores. Am J Physiol Endocrinol Metab 2003;285:E138–E154

17. Cha CY, Nakamura Y, Himeno Y, et al. Ionic mechanisms and Ca^{2+} dynamics underlying the glucose response of pancreatic β cells: a simulation study. J Gen Physiol 2011;138:21–37

18. Keizer J, Smolen P. Bursting electrical activity in pancreatic β cells caused by Ca^{2+}- and voltage-inactivated Ca^{2+} channels. Proc Natl Acad Sci U S A 1991;88: 3897–3901
19. Meyer-Hermann ME. The electrophysiology of the β-cell based on single transmembrane protein characteristics. Biophys J 2007;93:2952–2968
20. Tornheim K. Are metabolic oscillations responsible for normal oscillatory insulin secretion? Diabetes 1997;46:1375–1380
21. Tornheim K, Lowenstein JM. The purine nucleotide cycle. Control of phosphofructokinase and glycolytic oscillations in muscle extracts. J Biol Chem 1975;250: 6304–6314
22. Yaney GC, Schultz V, Cunningham BA, Dunaway GA, Corkey BE, Tornheim K. Phosphofructokinase isozymes in pancreatic islets and clonal β-cells (INS-1). Diabetes 1995;44:1285–1289
23. McKenna JP, Ha J, Merrins MJ, Satin LS, Sherman A, Bertram R. Ca^{2+} effects on ATP production and consumption have regulatory roles on oscillatory islet activity. Biophys J 2016;110:733–742
24. Dryselius S, Lund P-E, Gylfe E, Hellman B. Variations in ATP-sensitive K^+ channel activity provide evidence for inherent metabolic oscillations in pancreatic β-cells. Biochem Biophys Res Commun 1994;205:880–885
25. Nunemaker CS, Bertram R, Sherman A, Tsaneva-Atanasova K, Daniel CR, Satin LS. Glucose modulates $[Ca^{2+}]_i$ oscillations in pancreatic islets via ionic and glycolytic mechanisms. Biophys J 2006;91:2082–2096
26. Kennedy RT, Kauri LM, Dahlgren GM, Jung SK. Metabolic oscillations in beta-cells. Diabetes 2002;51(Suppl. 1):S152–S161
27. Bertram R, Satin LS, Pedersen MG, Luciani DS, Sherman A. Interaction of glycolysis and mitochondrial respiration in metabolic oscillations of pancreatic islets. Biophys J 2007;92:1544–1555
28. Merrins MJ, Fendler B, Zhang M, Sherman A, Bertram R, Satin LS. Metabolic oscillations in pancreatic islets depend on the intracellular Ca^{2+} level but not Ca^{2+} oscillations. Biophys J 2010;99:76–84
29. Ren J, Sherman A, Bertram R, et al. Slow oscillations of K_{ATP} conductance in mouse pancreatic islets provide support for electrical bursting driven by metabolic oscillations. Am J Physiol Endocrinol Metab 2013;305:E805–E817
30. Heart E, Smith PJS. Rhythm of the β-cell oscillator is not governed by a single regulator: multiple systems contribute to oscillatory behavior. Am J Physiol Endocrinol Metab 2007;292:E1295–E1300
31. Martin F, Sanchez-Andres JV, Soria B. Slow $[Ca^{2+}]_i$ oscillations induced by ketoisocaproate in single mouse pancreatic islets. Diabetes 1995;44:300–305
32. Dahlgren GM, Kauri LM, Kennedy RT. Substrate effects on oscillations in metabolism, calcium and secretion in single mouse islets of Langerhans. Biochim Biophys Acta 2005;1724:23–36
33. Lenzen S, Lerch M, Peckmann T, Tiedge M. Differential regulation of $[Ca^{2+}]_i$ oscillations in mouse pancreatic islets by glucose, α-ketoisocaproic acid, glyceraldehyde and glycolytic intermediates. Biochim Biophys Acta 2000;1523:65–72
34. Tantama M, Martínez-François JR, Mongeon R, Yellen G. Imaging energy status in live cells with a fluorescent biosensor of the intracellular ATP-to-ADP ratio. Nat Commun 2013;4:2550
35. Merrins MJ, Poudel C, McKenna JP, et al. Phase analysis of metabolic oscillations and membrane potential in pancreatic islet β-cells. Biophys J 2016;110:691–699
36. Li J, Shuai HY, Gylfe E, Tengholm A. Oscillations of sub-membrane ATP in glucose-stimulated beta cells depend on negative feedback from Ca^{2+}. Diabetologia 2013;56:1577–1586
37. Merrins MJ, Van Dyke AR, Mapp AK, Rizzo MA, Satin LS. Direct measurements of oscillatory glycolysis in pancreatic islet β-cells using novel fluorescence resonance energy transfer (FRET) biosensors for pyruvate kinase M2 activity. J Biol Chem 2013; 288:33312–33322
38. Denton RM. Regulation of mitochondrial dehydrogenases by calcium ions. Biochim Biophys Acta 2009;1787:1309–1316
39. Smolen P. A model for glycolytic oscillations based on skeletal muscle phosphofructokinase kinetics. J Theor Biol 1995;174:137–148
40. Keizer J, Magnus G. ATP-sensitive potassium channel and bursting in the pancreatic β cell. A theoretical study. Biophys J 1989;56:229–242
41. Markwardt ML, Seckinger KM, Rizzo MA. Regulation of glucokinase by intracellular calcium levels in pancreatic beta cells. J Biol Chem 2016;291:3000–3009
42. Richard A-MT, Webb D-L, Goodman JM, et al. Tissue-dependent loss of phosphofructokinase-M in mice with interrupted activity of the distal promoter: impairment in insulin secretion. Am J Physiol Endocrinol Metab 2007;293:E794–E801
43. Drews G, Bauer C, Edalat A, Düfer M, Krippeit-Drews P. Evidence against a Ca^{2+}-induced potentiation of dehydrogenase activity in pancreatic beta-cells. Pflugers Arch 2015;467:2389–2397
44. Düfer M, Haspel D, Krippeit-Drews P, Aguilar-Bryan L, Bryan J, Drews G. Oscillations of membrane potential and cytosolic Ca^{2+} concentration in $SUR1^{-/-}$ beta cells. Diabetologia 2004;47:488–498
45. Nenquin M, Szollosi A, Aguilar-Bryan L, Bryan J, Henquin JC. Both triggering and amplifying pathways contribute to fuel-induced insulin secretion in the absence of sulfonylurea receptor-1 in pancreatic β-cells. J Biol Chem 2004;279:32316–32324
46. Yildirim V, Vadrevu S, Thompson B, Satin LS, Bertram R. Upregulation of an inward rectifying K^+ channel can rescue slow Ca^{2+} oscillations in K(ATP) channel deficient pancreatic islets. PLOS Comput Biol 2017;13:e1005686
47. Hellman B, Dansk H, Grapengiesser E. Sulfonylurea blockade of KATP channels unmasks a distinct type of glucose-induced Ca^{2+} decrease in pancreatic β-cells. Pancreas 2017;46:467–475
48. Bertram R, Rhoads J, Cimbora WP. A phantom bursting mechanism for episodic bursting. Bull Math Biol 2008;70:1979–1993
49. Bertram R, Sherman A. A calcium-based phantom bursting model for pancreatic islets. Bull Math Biol 2004;66:1313–1344
50. Diederichs F. Mathematical simulation of membrane processes and metabolic fluxes of the pancreatic β-cell. Bull Math Biol 2006;68:1779–1818